Least-squares Wave-Equation Migration for Broadband Imaging

S. Lu (Petroleum Geo-Services), X. Li (Petroleum Geo-Services), A. Valenciano (Petroleum Geo-Services), N. Chemingui* (Petroleum Geo-Services), C. Cheng (UC-Berkeley)

Summary

We introduce an efficient Least-Squares Wave-Equation Migration (LS-WEM) for broadband imaging of seismic data. The procedure poses depth migration as an inversion problem. It is capable of producing high-resolution images of the subsurface corrected for overburden effects, variations in illumination, and incomplete acquisition geometries. The modeling engine for the inversion is an anisotropic one-way wave-equation extrapolator able to efficiently propagate high frequency seismic data using high-resolution earth models (e.g. derived from Full Waveform Inversion). The LS-WEM solves for the earth reflectivity in an iterative fashion through data space residual reduction. It integrates the anisotropic wavefield extrapolation operator with a fast linear inversion solver in an efficient migration/demigration algorithm. The algorithm produces high resolution images with high amplitude and structural fidelity. Applications of LS-WEM to synthetic and field data examples (from the Gulf of Mexico and the North Sea) consistently delivered higher resolution images compared to standard seismic migration.

Introduction

Depth migration produces a blurred representation of the earth reflectivity, with biased illumination and limited wavenumber content. The image resolution at a given depth is controlled by the acquisition parameters (source signature, frequency bandwidth, acquisition geometry), the earth properties at the reflector depth, the overburden (velocity, illumination and attenuation), and the migration operators. Some of these conditions can be mitigated during acquisition and processing by employing technologies like: multi-sensor data, full azimuth acquisition geometries, deghosting, attenuation compensation and using high-resolution earth models during depth migration (i.e. models derived from Full Waveform Inversion). However, in practice, where heterogeneities are present in the earth overburden and where the acquisition geometry leads to insufficient source and receiver coverage on the surface, both the illumination and wavenumber content of the depth-migrated images can be significantly restricted.

The illumination and resolution of the depth images can be improved by posing the imaging problem in terms of least squares inversion. The Least-Squares Migration (LSM) solutions (Schuster, 1993; Nemeth et al., 1999; Prucha and Biondi, 2002) are designed to produce images of the subsurface corrected for wavefield distortions caused by acquisition and propagation effects. They implicitly solve for the earth reflectivity by means of data residual reduction in an iterative fashion, which usually demands intensive computation. In seismic exploration framework, Nemeth et al. (1999) derived a Least-Squares Migration following a high-frequency Kirchhoff integral asymptotic approximation (ray-based). After, Prucha and Biondi (2002) derived less restrictive broadband wave-equation based solutions. The advantage of broadband wave-equation extrapolators is that they better utilize high-resolution/high contrast earth models derived with advanced processing technologies such as Full Waveform Inversion – FWI (Korsmo et al., 2017).

Here, we implement the LSM using an accurate anisotropic one-way wave-equation operator (Valenciano et al., 2011). Our application integrates this one-way operator with a fast linear inversion solver in an efficient migration/demigration workflow, namely a Least-Squares one-way Wave-Equation Migration (LS-WEM). Applications of LS-WEM to both synthetic and field data examples demonstrate improvements to the amplitude fidelity of the resulting image and enhancements to both temporal and spatial image resolution.

Methodology

Seismic imaging can be posed as a linearized inversion problem, where the unknown is the earth reflectivity $\boldsymbol{m}$ and the given are the observed data $\boldsymbol{d_{obs}}$. Historically, the adjoint solution to that problem (migration) has been used to estimate the earth reflectivity $\boldsymbol{m}$ as:

$$\boldsymbol{m} = \boldsymbol{L}^T \boldsymbol{d_{obs}} \quad , \qquad (1)$$

where $\boldsymbol{L}$ represents the linearized (Born) modeling operator, and its adjoint $\boldsymbol{L}^T$ is the migration operator. However, the heterogeneity of the overburden and/or limitations of the acquisition geometry can affect the illumination and wavenumber content of the estimated image $\boldsymbol{m}$.

A better approximation of the earth reflectivity is obtained by using least squares inversion, which solves a minimization problem to approximate the true reflectivity $\boldsymbol{m}$ as:

$$\boldsymbol{m} = \boldsymbol{argmin_m} \frac{1}{2} \| \boldsymbol{d_{obs}} - \boldsymbol{Lm} \|_2^2 \quad , \qquad (2)$$

In this case the acquisition geometry which relates to the operator $\boldsymbol{L}$ less affects the resulting image $\boldsymbol{m}$.

Here we introduce an implicit method to solve the Least-Squares problem. The LSM simulates data by wave-equation Born modeling, and iteratively updates the reflectivity by migration of the misfits between observed and simulated data. The algorithm can be summarized by the diagram in Figure 1 in an iterative modeling/migration framework. The first step of the flow is to produce an approximate reflectivity (migration). In the next step, the reflectivity is used for Born modeling. When the data residual $\| \boldsymbol{d_{obs}} - \boldsymbol{d_{mod}} \|$ is large, it is migrated to update the image $\boldsymbol{m}$. The inversion converges when the

simulated data matches the observation. One iteration (blue loop in Figure 1) comprises one Born modeling and one migration.

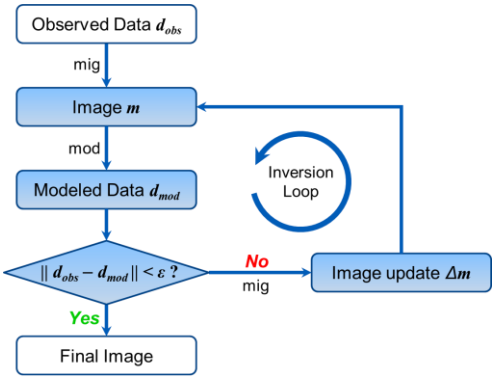

***Figure 1**: An iterative LSM algorithm solves for the earth reflectivity **m**. It simulates synthetic data $\mathbf{d}_{mod}$ by using a Born modeling operator, and iteratively update the reflectivity image **m** using migration of the data residual $\|\mathbf{d}_{obs} - \mathbf{d}_{mod}\|$.*

The computational cost of the iterative LSM relies on the efficiency of the wavefield propagation algorithm. Here, we implement the migration inversion using a one-way wave-equation operator (Valenciano et al., 2011), which has advantages of both accuracy and efficiency. In addition, our implementation combines the one-way extrapolator with fast linear inversion solvers into an efficient migration inversion system.

Synthetic and field data examples

We have performed a LS-WEM experiment using the 2D Sigsbee2b synthetic model [Figure 2]. The migration result [Figure 2A] shows uneven illumination from left sedimentary to subsalt area, including shadow zones (circled) related to the complex salt structures. LS-WEM improves the illumination by balancing the image amplitudes and reducing the effects of the shadow zones [Figure 2B]. It also enhances temporal resolution by broadening the frequency spectrum [Figure 2F]. Figure 2D and 2E show that LS-WEM balances the wavenumber content, improving the image of the faults and dipping salt flacks (indicated by arrows). In addition, LS-WEM converges rapidly to the true solution, reducing the data residuals by 90% in only four iterations [Figure 2G].

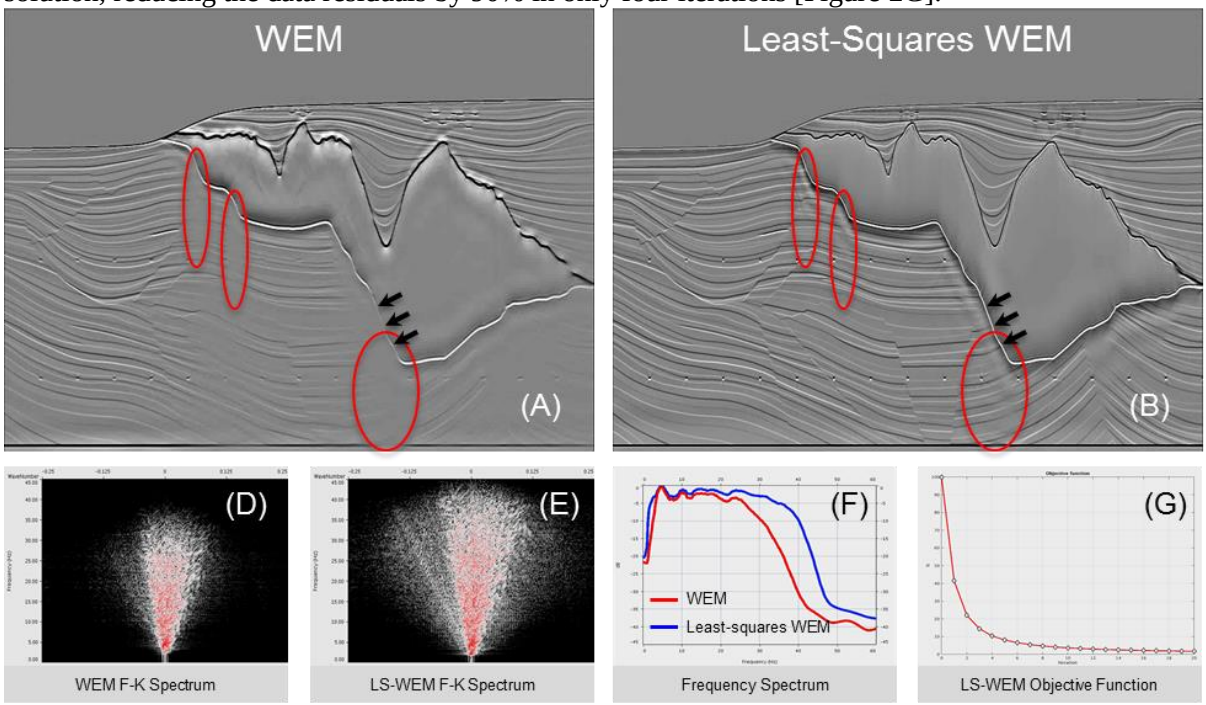

***Figure 2**: Sigsbee2b 2D synthetic example: (A) WEM image; (B) LS-WEM image; (D) F-K spectrum of WEM; (E) F-K spectrum of LS-WEM; (F) Frequency spectra of WEM [red] and LS-WEM [blue]; (G) LS-WEM objective function convergence rate.*

We also applied the LS-WEM to a wide azimuth data (WAZ) from the Gulf of Mexico. The results demonstrate that LS-WEM can deliver superior images compared to the standard migration [Figure 3 and 4]. The image improvements of LS-WEM over the standard migration can be summarized as: reduction of sail line acquisition footprint (lateral stripes indicated by arrows in Figure 3A), better resolution, and improved wavenumber content [Figure 3C, 3D and 3E]. The LS-WEM solution produces a better image of the fault planes (circled in Figure 4D). The inline and crossline sections [Figure 4] also reveal the improved wavenumber content.

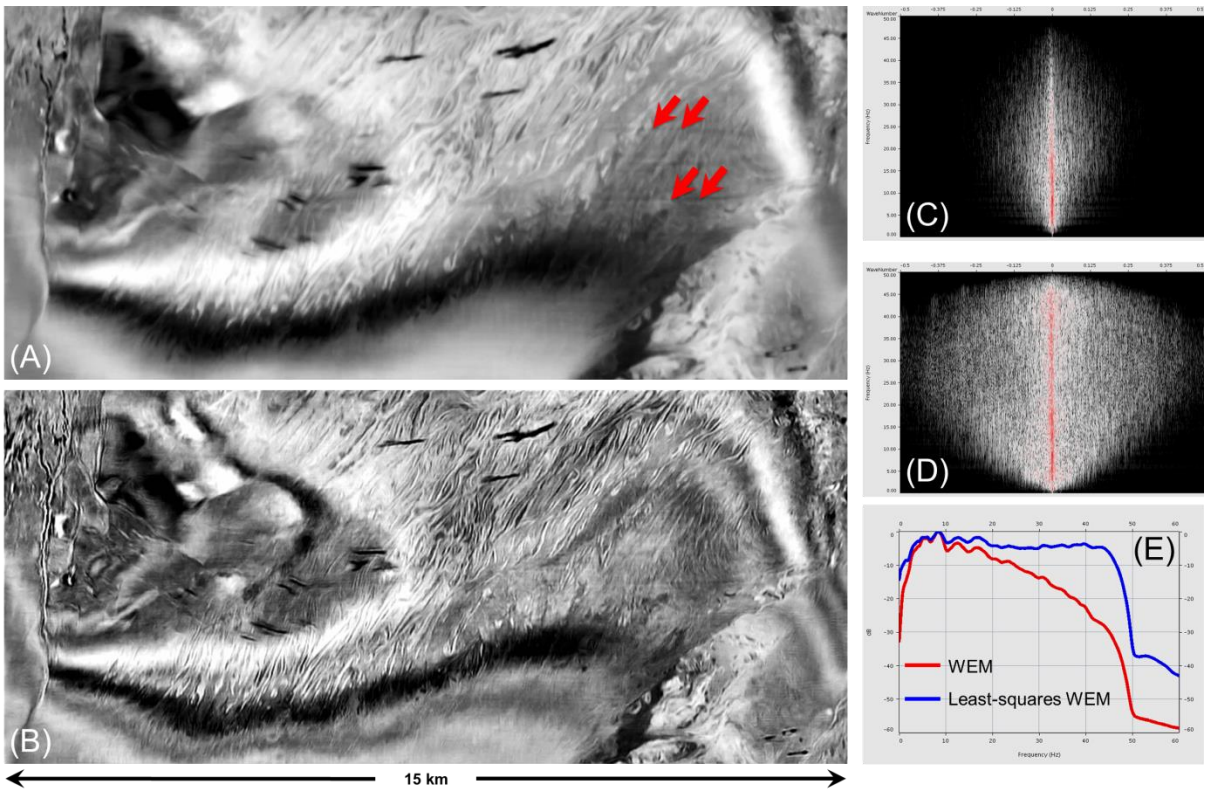

***Figure 3**: Gulf of Mexico 3D WAZ field data example: (A) Depth slice at 1150m from WEM; (B) Depth slice at 1150m from LS-WEM; (C) WEM F-K spectrum; (D) LS-WEM F-K spectrum; (E) Frequency spectra of WEM and LS-WEM.*

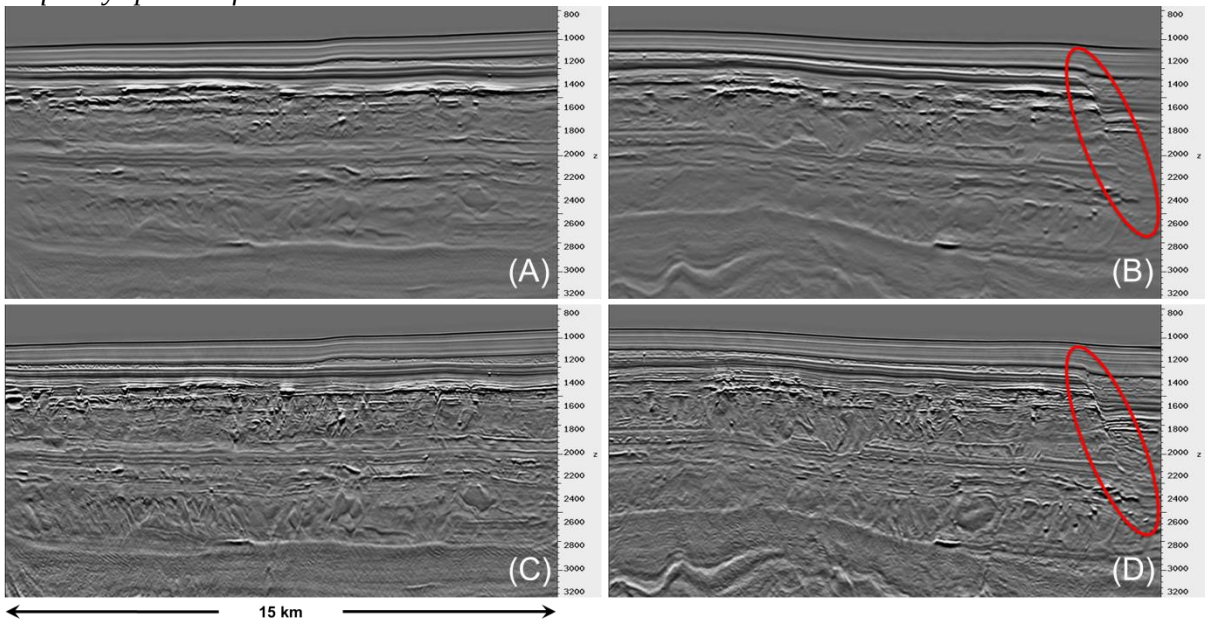

***Figure 4**: Gulf of Mexico 3D WAZ field data example: (A) WEM inline image; (B) WEM crossline image; (C) LS-WEM inline image; (D) LS-WEM crossline image.*

Another example of 3D narrow azimuth (NAZ) data from North Sea further illustrates the advantages of the LS-WEM. Figure 5 shows a comparison of the results from WEM and LS-WEM. The standard migration images are corrupted by the acquisition footprints, a typical problem of shallow water environment. The LS-WEM solution effectively reduces the acquisition footprint leading to a more interpretable image. The LS-WEM solution also improves the resolution as being illustrated in the first two examples.

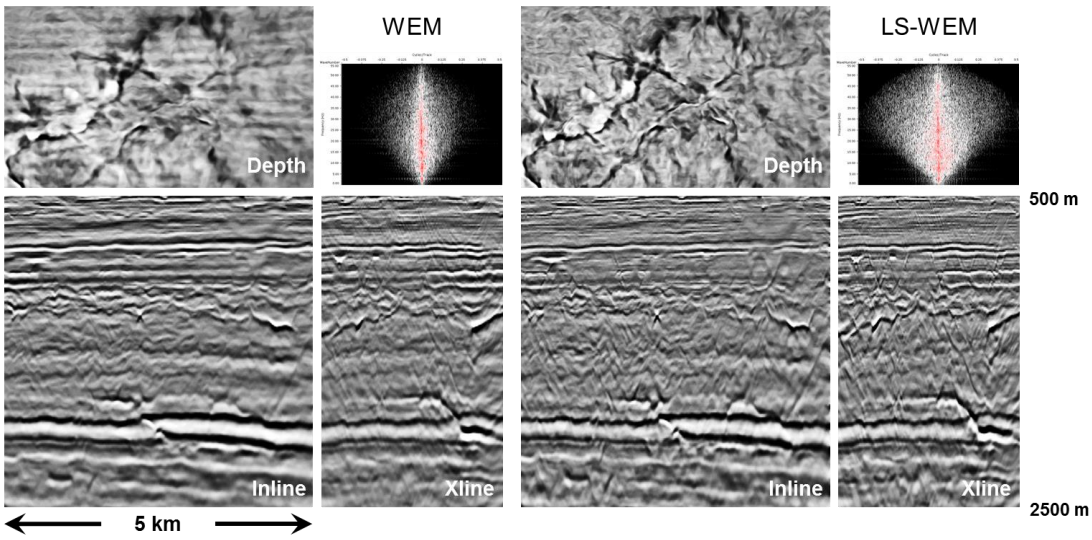

Figure 5*: North Sea 3D NAZ field data example. Left: WEM results; Right: LS-WEM results. The depth slice is at 1.8km.*

Conclusions

We introduce an efficient iterative Least-Squares Wave-Equation Migration (LS-WEM) solution for broadband imaging. The Least-Squares Migration is implemented using a one-way wave-equation wavefield propagator, which is able to fully utilize both the broader seismic bandwidth and the high-resolution velocity information from FWI. Our implementation combines the one-way extrapolator with fast linear inversion solvers into an efficient migration inversion system. LS-WEM application to both synthetic and field data demonstrate its ability to generate high-resolution images with better balanced amplitudes, broader frequency bandwidth and larger wavenumber content.

Acknowledgements

The authors thank PGS for permission to publish this work and for the approval to show the Multi-Client Gulf of Mexico data. We are also grateful to Aker BP for permission to publish the North Sea results. Furthermore, we thank Øystein Korsmo and Grunde Rønholt for supports and valuable discussion during the North Sea project.

References

Korsmo, Ø., O. J. Askim, Ø. Runde, and G. Rønholt, 2017, High fidelity velocity model building, imaging and reflectivity inversion - A case study over the Viking Graben area, Norwegian North Sea: 79th EAGE Conference & Exhibition.

Nemeth, T., C. Wu, and G. Schuster, 1999, Least-squares migration of incomplete reflection data: Geophysics, 64, 208–221.

Prucha, M. and B. Biondi, 2002, Subsalt event regularization with steering filters: 72th Annual International Meeting, Expanded Abstracts, 922–925, Soc. Expl. Geophysics.

Schuster, G., 1993, Least-squares crosswell migration: 63rd Annual International Meeting, SEG, Expanded Abstracts, 110–113.

Valenciano, A. A., N. Chemingui, D. Whitmore, and S. Brandsberg-Dahl, 2011, Wave equation migration with attenuation compensation: 73rd EAGE Conference & Exhibition.